Separation Science and Technology
Publication details, including instructions for authors and subscription information:
http://www.informaworld.com/smpp/title~content=t713708471

An Isotachophoretic Model of Counteracting Chromatographic Electrophoresis (CACE)

Jean B. Hunter[a]
[a] DEPARTMENT OF AGRICULTURAL AND BIOLOGICAL ENGINEERING, CORNELL UNIVERSITY, ITHACA, NEW YORK

To cite this Article Hunter, Jean B.(1988) 'An Isotachophoretic Model of Counteracting Chromatographic Electrophoresis (CACE)', Separation Science and Technology, 23: 8, 913 — 930
To link to this Article: DOI: 10.1080/01496398808063144
URL: http://dx.doi.org/10.1080/01496398808063144

SEPARATION SCIENCE AND TECHNOLOGY, 23(8 & 9), pp. 913-930, 1988

An Isotachophoretic Model of Counteracting Chromatographic Electrophoresis (CACE)

JEAN B. HUNTER

DEPARTMENT OF AGRICULTURAL AND BIOLOGICAL ENGINEERING
CORNELL UNIVERSITY
ITHACA, NEW YORK 14853

Abstract

Counteracting chromatographic electrophoresis (CACE) is a new electrophoretic technique for preparative separation of charged macromolecules, particularly proteins. CACE combines gel chromatography of a protein sample in a packed bed of gel beads having a gradient of exclusion limit, simultaneously with electrophoresis in an electric field tending to move the protein upstream. The target protein's convective movement opposes its electrophoretic movement, focusing the protein into an accumulation zone where its net velocity is zero. A mathematical model of concentrations and electrical fields in CACE was derived from an analogy to isotachophoresis. Accumulation-zone concentrations, electrical field, and pH were calculated from the bulk flow and electrophoretic fluxes of the target protein and buffer constituents, along with expressions for charge conservation and electroneutrality. The model predicts conditions for formation of protein accumulation zones given column operating parameters and mobility data for the target protein. Operating conditions correspond with available data on the CACE process, but calculated protein concentration was lower than that found experimentally.

INTRODUCTION

Chromatographic electrophoresis (*1*) is based on the observation that while a protein molecule's chromatographic velocity in a bed of size-exclusion gel beads is a strong function of exclusion limit, its electrophoretic velocity in such gels is nearly independent of exclusion limit. This disparity means that in a single column with uniform buffer flow

rate and uniform imposed electrical field, proteins may be made to migrate at different net rates in different portions of the column.

The mechanism of accumulation-zone formation can best be visualized by considering a column with a discontinuity in molecular-weight exclusion limit, as shown in Fig. 1. A column is packed with two different size-exclusion gels; a "tight" gel with a low exclusion limit near the column inlet, followed by a looser gel with higher exclusion limit. Hence a protein molecule will chromatograph more quickly through the first half of the column than the second. The electrical field applied to the column tends to move the protein molecules upstream against the flow. When the electrical field is properly adjusted, the target protein will move downstream in the first half of the column, and upstream in the second half, focusing in an accumulation zone (A-zone) at the interface between the two gels. The high concentration of negatively charged protein in the accumulation zone leads to a buildup of counterions, and the resulting increase in electrical conductivity lowers the local electric field until the equilibrium protein velocity in the zone is zero (*1*). As a consequence, protein added to a zone accumulates downstream of the interface, in the region of the gel with the higher exclusion limit.

CACE is exclusively a preparative method because it requires *a priori*

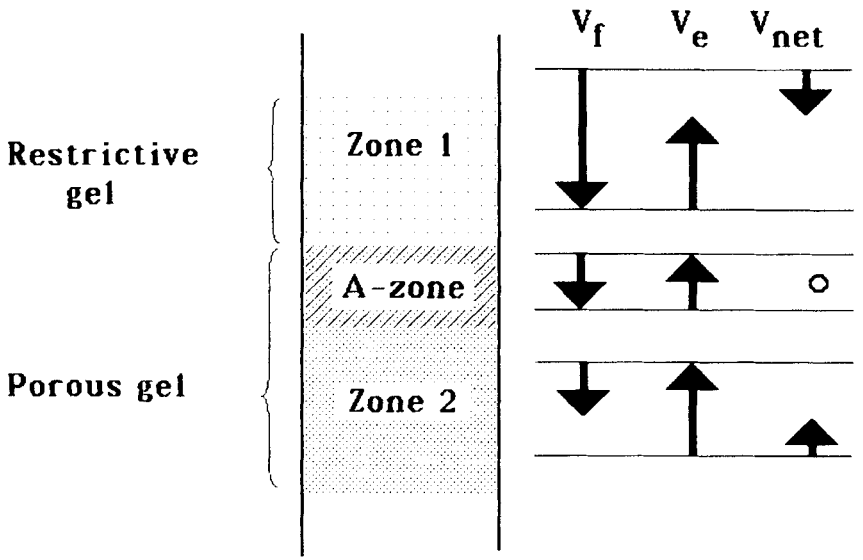

FIG. 1. Principle of accumulation-zone formation: Velocity balance on target protein.

knowledge of the target protein's electrophoretic and chromatographic mobilities in order to set operating conditions for accumulation of the target protein alone in the zone.

CACE's possible advantages over other preparative electrophoretic methods are concentration of the protein as well as separation, and the possibility of continuous operation in a one-dimensional system, by continuously withdrawing fluid from the accumulation zone. CACE may also be operated batchwise by building up a very long accumulation zone which is then eluted either electrophoretically or chromatographically. It appears particularly appropriate for recovery of extremely dilute proteins or of minor components of protein mixtures. Unlike isoelectric focusing, CACE is applicable to proteins having extreme pI's, and since it operates away from the pI, isoelectric precipitation is minimized. Disadvantages include high heat loads and low throughput, at least using existing "soft" size-exclusion gels. The protein components to be separated must also be stable and soluble at low ionic strength, since buffer conductivity must be kept as low as possible to minimize heating. The method seems best suited to production on a scale of 0.1 to 100 g purified protein per day; it is limited on the high end by heat transfer and continuous recovery problems associated with large-diameter columns, and on the low end by competition with HPLC and currently available continuous-flow electrophoretic methods.

GENERAL MODEL CONSIDERATIONS

A recent article by McCoy (*2*) addressed the problem of computing component velocities and accumulation-zone bandwidths in CACE and other imposed-gradient separation processes. Equations were derived for the net velocity of sample components subject to both partition and adsorption effects on the chromatographic matrix. The method of moments was used to compute the column position and peak width of a sample band migrating in a CACE column, both during transit to the gel interface and at equilibrium. By this analysis, the concentration profile of the accumulation zone is a composite of two exponential decay functions, meeting at a sharp point at the gel interface and trailing away on either side. The width of each portion of the zone depends on the dispersion coefficient for the protein in the column and on the magnitude of the restoring forces (net protein velocities) on each side of the interface. Similar expressions were proposed for the case in which the graduated property (here, matrix porosity) varied continuously rather than dis-

cretely. The model is limited by its assumption of a uniform electrical field throughout the column to the case of extremely low protein loads where accumulated protein does not affect the electrical field inside the A-zone.

In this report, CACE is modeled as a special case of isotachophoresis (ITP) against a counterflowing buffer stream. In ITP a mixture of anions (or cations) with a common counterion, bounded by a highly mobile "leader ion" and a "trailer ion" of low mobility, separate into adjacent zones under the influence of an electrical field. After steady state is achieved, each zone contains a single anionic (or cationic) species and the counterion, and all zones move at the same speed along the electrical potential gradient. In analytical applications a counterflow of buffer is often imposed on the system in order to immobilize the zones.

The CACE model is based on analogy to steady-state ITP, considering the protein accumulation zone to be similar to an isotachophoretic zone moving against a counterflow. The principal departure from ordinary ITP arises because of the different average convective velocities of macromolecules and ions. In CACE the counterflow is effectively larger for protein species than it is for buffer ions because of the gel sieving effect.

In this work a material- and charge-balance approach (*3*, *4*) is combined with expressions for protein valence and electrolyte dissociation equilibria to calculate A-zone conditions. Boundaries between zones in ITP are sharp and stable; hence it is assumed that the dispersive effects of diffusion and electroosmosis may be neglected, and that no field or concentration gradients exist within individual zones. When the ionic species are weak electrolytes, dissociation equilibria result in pH differences between the zones (*4*). Following these earlier workers, we neglect "end effects" of electrodes on buffer composition: it is sufficient to assume that the electrode buffer is inexhaustible, and that migration of electrode buffer ions does not affect the composition of the carrier buffer.

The model is developed for steady-state maintenance of a zone already formed and containing one protein. All of the protein is assumed to be located in the A-zone; only buffer components and water are present in the upper and lower zones. The electrolyte species in the buffer are treated as weak acids or weak bases. (Strong electrolytes may be modeled by setting the pK_a to extremely low or high values.) Mobilities of buffer ions vary with ionic strength according to the Debye-Huckel theory, but their mobility ratios are constant (*5*). All low molecular weight species are considered to be completely included within the gel.

The protein is considered to be a very large ion with a given intrinsic electrophoretic mobility based on its Stokes radius, and a charge that varies linearly with pH, being zero at the protein's isoelectric point. In this work the intrinsic mobility of the protein is considered to be independent of the gel media and ionic strength. The colloidal character of the protein is neglected except for its molecular sieving behavior.

The protein's pI and charge-to-pH proportionality may be determined by isoelectric focusing and titration, respectively. The effective void volume of a gel with respect to the target protein is easily calculated from the protein's elution volume on a column of that gel. Other inputs to the model are the composition and pH of the carrier buffer, the buffer flow rate, and the current density. These parameters are related to the operating conditions and are set by the experimenter.

CONSTRUCTION OF MODEL EQUATIONS

For a buffer system with M weak electrolyte constituents, the model requires determination of $(2M + 4)$ unknowns: the concentrations of the charged and uncharged species of each buffer constituent, the accumulation-zone pH, the concentration and charge of the target protein, and the electrical field inside the zone. A solution requires $(2M + 4)$ equations: M material balances on electrolyte constituents, M dissociation equilibria for the electrolytes, a velocity balance for the zero net velocity of the target protein inside the A-zone, an equation relating protein charge to pH, a conservation-of-current expression, and the constraint of local electroneutrality.

Titration curves show that the relationship of protein charge to pH is often fairly linear within 3 to 4 pH units of the pI of the protein, so we use the expression

$$z_p = r(\mathrm{pI} - \mathrm{pH}) \tag{1}$$

where z_p is the valence, considered dimensionless. The protein charge is positive when pH < pI and negative when pH > pI. The constant r is intrinsic to each protein and varies little with ionic strength above an ionic strength of about 0.02 (*6*).

The electrical field within the accumulation zone is determined by the zero net velocity of the protein within it. The protein's chromatographic velocity is

$$V_{fp} = V_f/\varepsilon_2 \tag{2}$$

where V_f is the superficial velocity of the carrier buffer and ε_2 is the fraction of the column volume (or cross-sectional area) accessible to the protein in the lower gel. For a totally excluded protein, ε is the void fraction of the column, 0.423 (*7*); for a totally included species, ε approaches 1.

The protein's electrophoretic velocity is

$$V_{ep} = E_a w_p z_p \tag{3}$$

where E_a is the electrical field (V/cm) within the accumulation zone, w_p is the intrinsic electrophoretic mobility of the protein ($cm^2/v \cdot s$ per unit valence), and z_p is determined by Eq. (1). At the field strength where $V_{fp} = -V_{ep}$, the protein's net velocity is zero, and

$$E_a = -V_f/(z_p w_p \varepsilon_2) \tag{4}$$

A more general analysis of the chromatographic velocity V_{fp} in CACE is given by McCoy (*2*).

Dissociation equilibria for the buffer ions, along with electroneutrality, set the pH in the accumulation zone. The ionized fraction α_i of a buffer constituent is a function of pH and is related to the pK_a of the constituent. For bases,

$$\alpha_k = H^+/(K_{ak} + H^+) \tag{5}$$

For acids,

$$\alpha_k = K_{ak}/(K_{ak} + H^+) \tag{6}$$

where K_{ak} is the dissociation constant of constituent k, $10^{-(pK_a)}$. Since the pH of the A-zone ordinarily differs from the pH in the outer zones, $\alpha_{ak} \neq \alpha_{2k}$. The ionized fraction of each constituent is the only portion carried along by electrophoresis, while both charged and uncharged species are convected at the buffer flow velocity.

Consider a mass balance for each component in the system. Let us define a column element bounded by two planes cutting across the column, one in the A-zone, and one in the lower section, Zone 2. All accumulation terms in a mass balance over this element must be set to zero, since the flux of each buffer constituent is constant throughout the column. The flux of constituent k through the upper plane is

$$J_{ak} = V_f c_{ak} + E_a c_{ak} w_k z_k \alpha_{ak} \tag{7}$$

where c_{ak} is the concentration of constituent k in the accumulation zone, w_k is the ion's intrinsic mobility, and z_k is the valence of the ionized form of constituent k. All buffer ions are convected at velocity V_f since they are too small to be affected by molecular sieving. The flux through the lower plane is

$$J_{2k} = V_f c_{2k} + E_2 c_{2k} w_k z_k \alpha_{2k} \tag{8}$$

where c_{2k} is the concentration of constituent k in the lower zone and E_2 is the electrical field of the upper and lower zones. E_2 can be found from the given current density and by the conductivity of the buffer, which in turn can be calculated from its known composition and the temperature. Equating J_{ak} and J_{2k} yields c_{ak} for each buffer constituent:

$$c_{ak} = c_{2k}(V_f + E_2 w_k z_k \alpha_{2k})/(V_f + E_a w_k z_k \alpha_{ak}) \tag{9}$$

Protein concentration cannot be found from this equation since c_p is zero outside the accumulation zone.

The most general expression for passage of current by ionic carriers involves the linear velocity of the carriers,

$$i = F \sum_{k=1}^{P} \alpha_k c_k z_k V_k \tag{10}$$

where i is the current density, A/cm^2, F is the faraday constant (96,500 C/mol), $\alpha_k c_k$ is the concentration of the ionized form of component k in mol/cm^3, and V_k is the local net linear velocity of component k, cm/s. Concentrations ($\alpha_k c_k$) of the water ions H^+ and OH^- are calculated from the pH of the solution and the dissociation constant of water, $K_w = 10^{-14}$ mol^2/L^2. Neglecting diffusion, $V_k = V_f + E_a w_k z_k$ for all buffer ions inside the A-zone, and the protein's net velocity V_p is zero. In free solution, bulk flow does not affect current because the convective velocity term V_f drops out due to electroneutrality. In this analysis it does not drop out since the convective velocity of the protein is V_f/ε_2, different from the velocity of the microions.

The electroneutrality constraint provides the means to calculate protein concentration in the A-zone. Since local charge density is everywhere zero,

$$\sum_{k=1}^{I} \alpha_{ak} c_{ak} z_k + c_p z_p = 0 \tag{11}$$

and

$$c_p = (-1/z_p) \sum_{k=1}^{I} \alpha_{ka} c_{ka} z_k \tag{12}$$

SOLUTION OF MODEL EQUATIONS

In theory, one may start with a given current density, buffer composition, and flow rate, and calculate pH and concentrations within the accumulation zone. In practice, it is easier to specify a zone pH, then calculate the current as a dependent variable, because the system then reduces to a system of linear algebraic equations. Afterwards one may iterate on pH to obtain results for the desired current density.

Our solution strategy was as follows: First the operating parameters were set: buffer composition, flow rate and pH, and ε values for gels. Next, the pH of the accumulation zone was specified and E_a calculated. E_2 then became a function of the unknown current density i ($E_2 = \kappa_2 i$) and the known conductivity of the outer zone. Finally, the equations for current density, protein concentration, and concentrations of buffer components were solved simultaneously.

Formulation of the linear solution matrix is presented here for a two-component buffer consisting of weak base T and weak acid S. The ionized constituents of T and S are denoted T^+ and S^-, respectively, and have valences $z_t = 1$ and $z_s = -1$.

The mass balance (Eq. 9) is rearranged as follows:

$$T_a^+/\alpha_{at} - (i/\kappa_2)T_2 w_t \alpha_{2t}/(V_f + E_a w_t \alpha_{at}) = T_2 V_f/(V_f + E_a w_t \alpha_{at}) \tag{13}$$

$$S_a^-/\alpha_{as} + (i/\kappa_2)S_2 w_s \alpha_{2s}/(V_f - E_a w_s \alpha_{as}) = S_2 V_f/(V_f - E_a w_s \alpha_{as}) \tag{14}$$

Electroneutrality becomes

$$T^+ - S^- + z_p c_p = (OH^-) - (H^+) \tag{15}$$

and the current balance

$$T^+(V_f + E_a w_t) - S^-(V_f - E_a w_s) - i(1000/F) = (OH^-)(V_f - E_a w_{(OH^-)}) - (H^+)(V_f + E_a w_{(H^+)}) \tag{16}$$

Rearranging this into matrix notation, $\mathbf{Ax} = \mathbf{y}$, where $\mathbf{x}^t$ is the row vector $[T^+, S^-, c_p, i]$, $\mathbf{A}$ is the matrix of coefficients, and $\mathbf{y}$ is the solution vector made up of the r.h.s. of the last four equations. The matrix $\mathbf{A}$ was inverted analytically. $\mathbf{A}^{-1}$ is sufficiently well-conditioned that excellent results were obtained using double precision arithmetic. Mobilities for buffer ions were taken from Jovin (*5*).

RESULTS

The model predicts conditions for successful formation of an accumulation zone, based on given mobility data, buffer composition, and flow rate. At any buffer flow velocity, the electrical field must be high enough to carry the protein upstream in the lower column section, yet low enough that the protein moves downstream in the upper column section. Hence a velocity balance in the upper and lower column zones determines current density values under which a zone may form. The maximum electrical field permissible is the value that will set V_{net} to zero in the upper zone. Similarly, we can calculate the minimum field strength from the limit of zero movement of the protein in the lower zone, using Eq. (4):

$$E_{max} = -V_f/(z_p w_p \varepsilon_1) \tag{17a}$$

$$E_{min} = -V_f/(z_p w_p \varepsilon_2) \tag{17b}$$

Since the conductivity of the buffer in the outer zones, κ, is given, we can calculate i_{max} and i_{min} as

$$i_{max} = -V_f \kappa/(z_p w_p \varepsilon_1) \tag{18a}$$

$$i_{min} = -V_f \kappa/(z_p w_p \varepsilon_2) \tag{18b}$$

Constraints of electroneutrality and constant flux dictate a second current density limit by requiring that all buffer constituents flow downstream in all parts of the column. In the case of acidic buffer electrolytes, anions are moved upstream by the electric field, while both charged and uncharged species are carried downstream by buffer flow. If electroneutrality is to hold within the A-zone, there must be a local excess of buffer cations over buffer anions in order to compensate for the added aconcentration of negatively charged protein. By rearrangement of Eq. (9), the ratio of ionized fractions of buffer constituent k in the A-zone and Zone 2 is found to be

$$\alpha_{ak}c_{ak}/\alpha_{2k}c_{2k} = (E_2/E_a) - V_f(E_2\alpha_{2k} - E_a\alpha_{ak})/[E_a\alpha_{2k}(V_f + E_a w_k z_k \alpha_{ak})] \tag{19}$$

$E_2 > E_a$ and $\alpha_2 > \alpha_a$, so the numerator of the second term is positive. Since the denominator is always positive for cations, their concentration ratio is always lower than the ratio of electrical fields, but the concentration ratio for anions depends on the relative magnitudes of V_f and $E_a w_k \alpha_{ak}$. If $E_a w_k \alpha_{ak}$ exceeds V_f, then the anionic buffer constituent moves upstream in the A-zone. In this circumstance the ratio of anion concentrations in the two zones is greater than the ratio of electrical fields, leading to an excess of anions over cations in the A-zone. The condition surfaces mathematically as a negative protein concentration as the model tries to achieve electroneutrality. Experimentally, it leads to nearly complete dissipation of the accumulation zone and a rise in temperature. It can be shown that when $V_f > E_a w_k \alpha_{ak}$, there will always be an excess of buffer cations over anions in the A-zone. Finally, the steady-state assumption for buffer constituents requires that V_f also exceed $E_2 w_k \alpha_{2k}$, to prevent any buildup of buffer anions at the lower interface of the accumulation zone. Setting $V_f - E_2 w_k \alpha_{2k}$ equal to zero determines an alternate maximum value for current density,

$$i'_{max} = \kappa_2 V_f / w_s \alpha_{2s} \tag{20}$$

which may be greater or smaller than the i_{max} based on protein velocity balance (Eq. 18a). If the protein's intrinsic mobility or net charge is sufficiently low, i_{min} may exceed i'_{max}. This occurs when

$$z_p w_p \varepsilon_2 < \alpha_{2s} w_s \tag{21}$$

Under these conditions, formation of a tightly focused accumulation zone is impossible, and the problem electrolyte must be replaced with one having lower-mobility anions or a higher pK_a. In physical terms, a zone cannot form unless the electrophoretic mobility of the protein, $z_p w_p$, exceeds the average electrophoretic mobility of the anionic buffer constituent. Clearly it is necessary to have either a highly mobile protein or a very weakly dissociated buffer anion in order to form a zone.

A final constraint on operating conditions is Joule heating of the gel bed due to passage of electrical current. Little heat is removed from a conventionally sized column by the flowing buffer, so heat transfer is predominantly radial. (In our experience, cooling of a 0.7 cm i.d. column was necessary when heat loads exceeded about 0.1 W/cm^3.) More heat is

generated in the upper and lower column zones than in the accumulation zone, where the electrical field is lower. Although protein denaturation is possible at elevated temperatures, a more important problem is the narrowing of column operating limits due to radial temperature gradients. As a general rule, ionic mobilities increase 1.5 to 2%/°C; hence a 5°C temperature difference between column wall and centerline raises the centerline ionic mobilities by 7.2 to 11%. The effect on protein and anion velocity profiles is shown in Fig. 2. Therefore radial temperature gradients decrease i_{max} and i'_{max}.

The model was tested against published data (*1*) for the focusing of ferritin between Bio-Gel P-10 and A-50 gels (Bio-Rad Laboratories). Ferritin is a spherical molecule whose protein moiety has a molecular

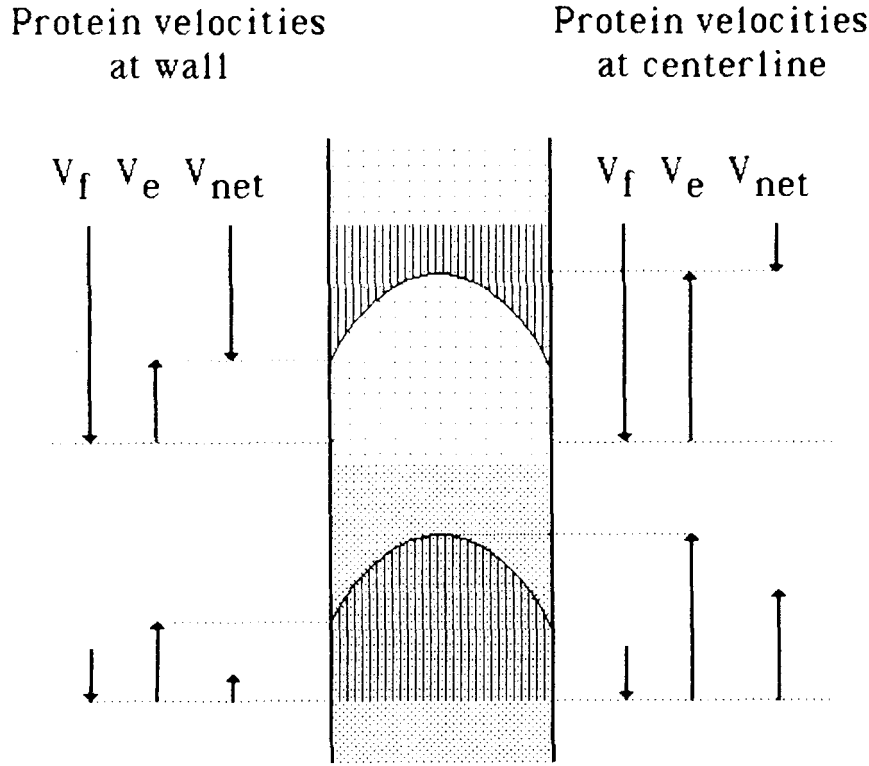

FIG. 2. Effect of radial temperature gradients on target protein velocity. The temperature dependence of electrophoretic mobility causes a difference in net protein velocity between the column wall and centerline.

weight of about 450,000 daltons. Its iron hydroxide core has no effect on its charge (*8*) or electrophoretic migration properties (*9*) which include size and shape. The Stokes radius of around 65 Å (*10*) provided a basis for estimating intrinsic mobility. Combining the Stokes-Einstein and Nernst-Einstein equations gives

$$w_p = F/6N\pi\mu a \tag{22}$$

where μ is buffer viscosity (g · cm/s), a is the Stokes radius (cm), and N is Avogadro's number (mol^{-1}). Using this method the intrinsic mobility of ferritin was calculated at 1.37×10^{-5} $cm^2/V \cdot s \cdot$ charge. This value is higher than literature values computed from measured and calculated free electrophoretic mobilities (*11*, *12*) and electrophoretically calculated valences which were in the range of 3.3 to 7.8×10^{-6} $cm^2/v \cdot s \cdot$ charge. The mobility was also estimated at 1.4×10^{-6} by analogy to ovalbumin, by calculating an intrinsic mobility for ovalbumin from titration and mobility data (*12*), then dividing it by the cube root of the molecular weight ratio (an estimate of the ratio of Stokes radii). A similar analogy for hemoglobin (*6*, *13*) gives a w_p value of 1.35×10^{-6}. A compromise value of 7.1×10^{-6} was used.

The isoelectric point of ferritin is 4.4 (*14*). The pH/charge proportionality constant r for ferritin, determined by titration at an unspecified but "very low" ionic strength, is around 150 charges/molecule per pH unit (*8*). The titration curve was quite linear over a pH range from 2 to 12. By analogy with hemoglobin, multiplying its titration r-value of about 8 (*6*) by the ratio of molecular weights, ferritin should have an r-value of 57.5 at ionic strengths of 0.02 and higher. Finally, valences calculated from electrophoretic mobilities in polyacrylamide gels at ionic strengths of 0.008 to 0.0015 give values of r on the order of 5 to 10 (*9*, *11*, *12*). The value based on hemoglobin was chosen as a compromise.

The buffer system was 10 m*M* Tris acetate pH 7.4, which we considered to comprise 10 m*M* Tris and 8.256 m*M* acetate. This formula has an ionic strength of 0.00824. Manufacturer's data (*15*) on Bio-gel P-10 and A-50 indicate that ferritin should be completely excluded from the P-10 gel and completely included in the A-50 gel. The accessible column volume ε_1 was thus set to 0.423 (*7*) and ε_2 to 1. The buffer flow rate was 7.3622×10^{-3} cm/s. The total potential drop over the 50-cm long column and the two electrode buffer chambers was reported as 600 V, measured at the power supply. If concentrated electrode buffers were used, the entire potential drop may be assumed to occur over the column. The outer-zone electrical field was then calculated as 12 V/cm, the current density 6.124

mA, and the heat load 73.5 mW/cm^3. Using these estimates to duplicate O'Farrell's conditions, the model predicted formation of an A-zone at pH 7.335, giving a protein concentration of 3.1054×10^{-5} *M* (14.285 g/L).

Except for protein concentration, O'Farrell's operating conditions fall into the operating range predicted by the model and shown in Figs. 3 and 4. Zone formation was predicted at current densities from 3.176 to 7.506 mA, corresponding to outer-zone electrical fields from 6.223 to 14.71 V/cm. The protein velocity balance determined the upper current-density limit of the operating range at pH 7.308. At an A-zone pH of 7.4, equal to the buffer pH, no protein accumulated and the current density was calculated as i_{min}. Figures 3 and 4 show c_p, A-zone pH, and the protein and buffer anion velocities as functions of the current density. Table 1 presents the above results for comparison with model predictions for different operating conditions. Simulations were run at pH 7 and 6.6 to determine the effect of buffer pH, at $\varepsilon_1 = 0.25$ to simulate a gel compressed by high flow rates, and at an elevated buffer concentration of 50 m*M* Tris acetate. Replacement of the Tris-acetate by a Tris-borate buffer was also modeled. The Table 1 entries for pH 6.6 for $\varepsilon_2 = 0.25$ and

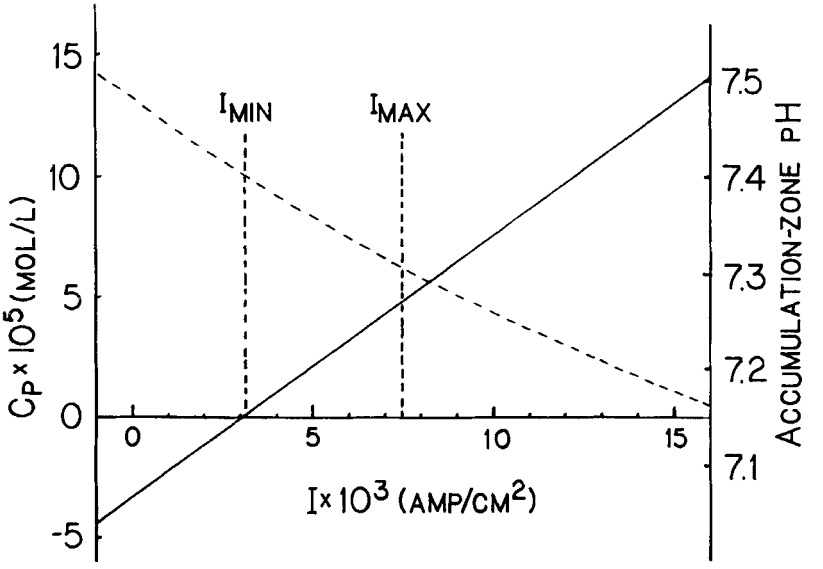

FIG. 3. Model predictions: Protein concentration c_p and pH in accumulation zone as a function of current density. Conditions of O'Farrell (*1*). An accumulation zone forms for current densities between i_{min} and i_{max}. (——) c_p; (- -) pH.

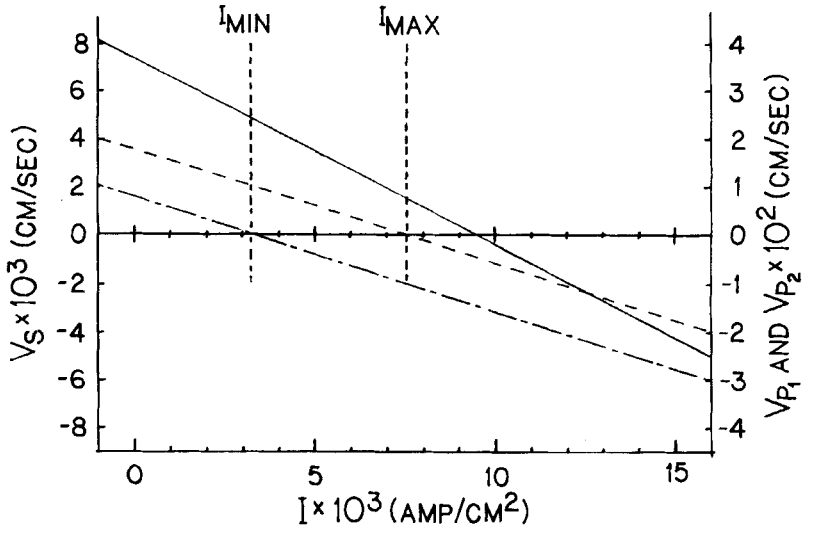

FIG. 4. Model predictions: Net velocity of protein in upper (V_{p1}) and lower (V_{p2}) column sections of net velocity of acetate ion (V_s) as functions of current density. A positive velocity denotes movement in the downstream direction. Conditions of O'Farrell (*1*). (——) V_s; (- -) V_{p1}; (— -) V_{p2}.

for the Tris-borate buffer are of particular interest since they demonstrate situations where buffer anion velocities limit current density, that is, where i'_{max} rather than i_{max} is the upper current limit for CACE operation.

DISCUSSION

The major discrepancy between this model and O'Farrell's experimental results is the predicted protein concentration in the accumulation zone. O'Farrell reported a ferritin concentration of around 130 g/L; the model predicts 14.285 g/L.

Given the spread in reported values for mobility and especially for valence, our estimates of intrinsic mobility and charge-pH dependence of ferritin may account for much of the discrepancy in protein concentration. Either a higher value of w_p or a lower z_p would increase the model's estimate of protein concentration. For example, cation binding by the negatively charged ferritin in the accumulation zone would decrease z_p without substantially affecting w_p. However, a value of $z_p w_p$ (protein

TABLE 1
Computed Current Density Limits, Power, and Ferritin Concentration for Different CACE Operating Conditions

Conditions	Power at $c_{p\text{-}max}$ (W/cm^3)	I_{min} (mA)	i_{max} (mA)	i'_{max} (mA)	Range of pH$_a$	$c_{p\text{-}max}$ mol/L × 10^{-5} g/L		κ (mho/cm × 10^{-4})
O'Farrell's conditions: tris-acetate 10 m*M*, pH 7.4, ε_1 = 0.423	.1097	3.176	7.506	9.532	7.308–7.4	4.596	21.14	5.1037
Tris-acetate 10 m*M*, pH 7.0, ε_1 = 0.423	.1653	4.109	9.713	10.96	6.879–7.0	7.412	34.09	5.6934
Tris-acetate 10 m*M*, pH 6.6, ε_1 = 0.423	.2086	5.128	12.12	11.32	6.312–6.6	11.14	51.25	5.9686
Tris-acetate 10 m*M*, pH 7.4, ε_1 = 0.25	.1770	3.175	12.70	9.532	7.266–7.4	6.884	31.66	5.1037
Tris-acetate 50 m*M*, pH 7.4, ε_1 = 0.423	.5186	15.03	35.54	47.66	7.312–7.4	21.33	98.1	24.162
Tris-borate 10 m*M*, pH 7.4, ε_1 = 0.423	.0282	2.736	6.470	677.8	7.19–7.4	3.396	15.62	4.3931
Tris-acetate 50 m*M*, pH 7.4, ε_1 = 0.25	.9365	15.03	60.13	48.12	7.266–7.4	34.84	160.3	24.162

electrophoretic mobility) below 3.95×10^{-4} cm^2/V · s, the mobility of the acetate constituent, would preclude zone formation. This value is disturbingly higher than mobility values reported in the literature, which are on the order of 10^{-4} cm^2/V · s (*11*).

Factors which tend to lower cation velocity relative to anion velocity inside the accumulation zone will increase the cation/anion concentration ratio, favoring a higher protein concentration. In the model, the relative mobilities w_k of the ions were presumed to be constant. In reality, their dependence on ionic strength is predicted by the Debye-Huckel-Onsager theory,

$$w_k/w_k^\circ = 1 - (A/w_k^\circ + B)I \tag{23}$$

where w_k° is the mobility at zero ionic strength, A and B are constants depending on the solvent and the valence of the ion, and I denotes ionic strength. The decrease in mobility with ionic strength is relatively greater for ions with low mobility (such as Tris) and less for more mobile ions (acetate, sulfate, chloride), and can result in changes in relative mobility of 10 to 20%. Both through counterion accumulation and the disproportionate effect of highly charged protein, high values of ionic strength are attained in the accumulation zone. Thus ionic strength effects on ion mobilities may be substantial.

Donnan equilibria at the anodic and cathodic interfaces of the A-zone are very likely to boost protein concentration. Two mechanisms apply: thermodynamically favored accumulation of cations and permselectivity. Both effects are most pronounced when buffer ionic strength is low and protein concentration is high (*16*). The motionless, negatively charged protein in the A-zone may be compared to a cation-exchange membrane in an electrodialysis apparatus. Such a membrane is far more permeable to cations than to anions, thus most of the current through the membrane is carried by cations, while anions accumulate on the upstream side. The electrodialysis analogy also predicts gradients in the pH profile around the "membrane" (*17*). The result is a region of low ionic strength, high pH, and high electrical field downstream of the A-zone, and a region of high ionic strength, low pH, and low field just upstream. The field and pH profile distortions simultaneously accelerate protein into the zone from both the upstream and downstream sides, compressing the zone into a smaller space and thereby increasing its protein concentration.

Although it is clear that these effects exist, it is difficult to make analytical predictions of their magnitude. A model incorporating thermodynamic and diffusional effects is now under development, using the approach developed by Palusinski and coworkers (*18*).

CONCLUSIONS

A simple steady-state model of CACE, developed by analogy to isotachophoresis, predicts formation of accumulation zones and the operating conditions necessary to achieve a compact zone. The model agreed with published results on conditions for focusing of ferritin, though it seriously underestimated protein concentration.

Successful operation of a CACE column depends on adjustment of the current density in the column to meet constraints on the velocity of the target protein and on buffer ions having the same valence sign as the target protein. Protein anywhere in the column must always move toward the interface, and all buffer constituents must have a net flux downstream.

Uncertainty in estimates of electrophoretic parameters, dependence of relative ion mobilities on ionic strength, or Donnan equilibria at zone boundaries are probably responsible for the extremely high protein concentrations found experimentally but not well predicted by the model.

GLOSSARY

c_{2k}	concentration of species k in upper and lower zones, mol/cm^3
c_{ak}	concentration of species k in accumulation zone, mol/cm^3
c_p	protein concentration, mol/cm^3
z_p	charge of protein ion: $z_p = r(\text{pI} - \text{pH})$, dimensionless
w_k	intrinsic electrophoretic mobility of species k, cm^2/(V · s · unit valence)
α_k	fraction of component k ionized
$\varepsilon_1, \varepsilon_2$	void fraction of upstream and downstream gels with respect to the target protein
E_a	electrical field inside accumulation zone, V/cm
E_2	electrical field in upper and lower zones, V/cm
i	current density, A/cm^2
V_f	linear velocity of buffer, cm/s
V_p	bulk-flow component of protein linear velocity, cm/s
V_e	electrophoretic component of protein velocity, cm/s
κ	electrical conductivity of buffer in upper and lower zones, mho/cm
D	diffusivity, cm^2/s
J_{ak}, J_{2k}	flux of component k in accumulation zone and outer zones, respectively, mol/cm^2 · s

Acknowledgments

The author wishes to express appreciation to B. J. McCoy, R. A. Mosher, C. F. Ivory, and P. H. O'Farrell for helpful discussions. This work was supported by a grant from the Cornell Biotechnology Program which is sponsored by the New York State Science and Technology Foundation, a consortium of industries, and the U.S. Army Research Office.

REFERENCES

1. P. H. O'Farrell, *Science, 227,* 1586 (1985).
2. B. J. McCoy, *AIChE J., 32,* 1570 (1986).
3. V. P. Dole, *J. Am. Chem. Soc., 67,* 1119 (1945).
4. E. B. Dismukes and R. A. Alberty, *Ibid., 76,* 191 (1954).
5. T. Jovin, *Ann. N. Y. Acad. Sci., 209,* 477 (1973) (table of mobilities, p. 482).
6. W. H. Orttung, *Biochemistry, 9,* 2394 (1970).
7. D. H. Kim and A. F. Johnson, in *Size Exclusion Chromatography: Methodology and Characterization of Polymers and Related Materials* (T. Provder, ed.), American Chemical Society, Washington, D.C., 1984, pp. 25–45.
8. T. Nakamura and K. Konno, *J. Biochem., 41,* 499 (1954).
9. L. Vulimiri, N. Catsimpoolas, A. L. Griffith, M. C. Linder, and H. N. Munro, *Biochim. Biophys. Acta, 412,* 148 (1975).
10. P. Aisen and I. Listowsky, *Ann. Rev. Biochem., 49,* 357 (1980).
11. P. Masson and J. Anguille, *J. Chromatogr., 192,* 402 (1980).
12. D. Rodbard and A. Chrambach, *Anal. Biochem., 40,* 95 (1971).
13. L. Pauling, H. A. Itano, S. J. Singer, and I. C. Wells, *Science, 110,* 543 (1980).
14. A. Mazur and E. Shorr, *J. Biol. Chem., 182,* 607 (1950).
15. *Chromatography, Electrophoresis, Immunochemistry, Molecular Biology, HPLC,* Bio-Rad Laboratories Price List M, April 1987.
16. N. Lakshminarayanaiah, *Transport Phenomena in Membranes,* Academic, New York, 1969, pp. 79–112 and 274–284.
17. M. Bier, O. A. Palusinski, R. A. Mosher, and D. A. Saville, *Science, 219,* 1281 (1983).
18. O. A. Palusinski, T. T. Allgyer, R. A. Mosher, M. Bier, and D. Saville, *Biophys. Chem., 13,* 193 (1981).